The Synthesis and Characterization of Two-Dimensional Ferromagnetic Extended Structures Containing High-Spin ($S = {}^5/_2$) and Low-Spin ($S = {}^1/_2$) Iron(III) Bridged by Cyanide Groups

Nazzareno Re

Dipartimento di Chimica, Università di Perugia, I-06100 Perugia, Italy

Raffaella Crescenzi and Carlo Floriani*

Institut de Chimie Minérale et Analytique, BCH, Université de Lausanne, CH-1015 Lausanne, Switzerland

Hitoshi Miyasaka

Department of Chemistry, Faculty of Science, Kyushu University, Hakozaki, Fukuoka 812, Japan

Naohide Matsumoto*

Department of Chemistry, Faculty of Science, Kumamoto University, Kurokami 2-39-1, Kumamoto 860, Japan

Received December 9, 1997

The reaction of $[Fe(salen)]^+$ and $\{A_3[Fe(CN)_6]\}$ (A = NEt_4, K), depending on the countercation A^+ and on the reaction solvent, led to $[(NEt_4)\{Fe(salen)\}_2\{Fe(CN)_6\}]_n$, **4**, and $[\{Fe(salen)\}_3\{Fe(CN)_6\}(MeOH)_2]_n \cdot 3nH_2O$, **5** [$NEt_4$ = tetraethylammonium cation, salen = *N*, *N*′-ethylenebis(salicylideneiminato) dianion], displaying a similar extended 2D structure. Complex **5** crystallizes in the monoclinic, space group $P2_1/n$, $a = 13.495(7)$ Å, $b = 14.220(9)$ Å, $c = 33.137(5)$ Å, $\beta = 96.74(2)°$, and $Z = 4$. It assumes a two-dimensional network layer structure consisting of cyclic octanuclear [-Fe(h.s.)-NC-Fe(l.s.)-CN-]$_4$ units with $[Fe(salen)(MeOH)_2]^+$ located between the interlayer as a countercation. Complex **4** exhibits a metamagnetic behavior with a field-induced transition from an antiferromagnetic to a ferromagnetic-like state and a Neel temperature of ca. 6 K.

Introduction

Much effort has been directed toward the design molecular-based magnetic materials exhibiting spontaneous magnetization, and particularly so for the synthesis of 2D- and 3D-like magnetic materials.[1−4] We recently reported a series of 2D magnetic materials, $[K\{Mn(3\text{-}MeOsalen)\}_2\{Fe(CN)_6\}(DMF)]_n$[5a,b] and $[(NEt_4)\{Mn(5\text{-}Clsalen)\}_2\{Fe(CN)_6\}]_n$,[5d] in which the two-dimensional network is made up of a cyclic octanuclear [-Mn-NC-Fe-CN-]$_4$ network unit. The magnetic behavior of such materials has been tuned through: (i) the changes in the Schiff base ligand; (ii) the nature of the countercation; and (iii) the change in the transition metal couple, as we illustrated in a series of two-dimensional compounds $[K\{Mn(3\text{-}MeOsalen)\}_2\{M(CN)_6\}]_n$ (M = Co^{3+}, $S = 0$; Fe^{3+}, $S = {}^1/_2$; Mn^{3+}, $S = 1$; and Cr^{3+}, $S = {}^3/_2$).[5]

We have extended this study by assembling the high-spin iron(III) ($S = {}^5/_2$) $[Fe(salen)]^+$ cation with the low-spin iron(III) ($S = {}^1/_2$) $[Fe(CN)_6]^{3-}$, via the reaction of [Fe(salen)(Cl)], **1**, with $\{A_3[Fe(CN)_6]\}$ (A = NEt_4, **2**; A = K, **3**). Depending on the countercation A, this reaction led to two different kinds of complexes, namely $[(NEt_4)\{Fe(salen)\}_2\{Fe(CN)_6\}]_n$, **4**, and $[\{Fe(salen)\}_3\{Fe(CN)_6\}(MeOH)_2]_n \cdot 3nH_2O$, **5** [$NEt_4$ = tetraethylammonium cation, salen = *N*,*N*′-ethylenebis(salicylideneiminato) dianion]. Complex **4** exhibits metamagnetic behavior with a field-induced transition from an antiferromagnetic to a ferromagnetic-like state. The purpose of this article is to report their syntheses, crystal structures, and magnetic properties.

Experimental Section

Physical Measurements. Elemental analyses for C, H, and N were performed at the Elemental Analysis Service Center of Kyushu University. Iron analyses were made on a Shimadzu AA-680 atomic absorption/flame emission spectrophotometer. Infrared spectra were measured on KBr disks with JASCO IR-810 and Shimadzu FTIR-8600 spectrophotometers. Thermogravimetric analyses (TGA) were carried out on a Rigaku Denki TG-DTA apparatus, with a heating rate of 1.25 °C/min and a temperature range 20−300 °C. Magnetic susceptibilities were finally measured at Lausanne University using an MPMS5 SQUID susceptometer (Quantum Design Inc.); the applied magnetic fields were 600−800 G, and the calibrations were made with with $(NH_4)_2Mn$-

* Corresponding authors.

(1) (a) Abrahams, B. F.; Hoskins, B. F.; Michail, D. M.; Robson, R. *Nature* **1994**, *369*, 727. (b) Batten, S. R.; Hoskins, B. F.; Robson, R. *Angew. Chem., Int. Ed. Engl.* **1995**, *34*, 820. (c) Yaghi, O. M.; Li, G.; Li, H. *Nature* **1995**, *378*, 703. (d) Yaghi, O. M.; Li, H. *J. Am. Chem. Soc.* **1996**, *118*, 295. (e) Real, J. A.; Andrés, E.; Munoz, M. C.; Julve, M.; Granier, T.; Bousseksou, A.; Varret, F. *Science* **1995**, *268*, 265.

S0020-1669(97)01544-9 CCC: $15.00
Published on Web 05/02/1998

$(SO_4)_2 \cdot 6H_2O$ for the SQUID susceptometer.[6] Field dependency measurements with magnetization up to 5.5 T were made on a MPMS5 SQUID susceptometer (Quantum Design Inc.). Corrections were applied for diamagnetism calculated from Pascal's constants.[7]

X-ray Data Collection, Reduction, and Structure Determination. Single crystals were prepared by the method described in the synthetic procedure. The single crystal for the crystallographic analysis was cut from a thin plate crystal and sealed in Lindemann glass capillaries. Crystal dimensions are 0.35 × 0.07 × 0.40 mm. All measurements were made on Rigaku AFC7R diffractometer with graphite-monochromated Mo Kα radiation ($\lambda = 0.710\ 69$ Å) and a 12 kW rotating anode generator. The data were collected at a temperature of 20 ± 1 °C using $\omega-2\theta$ scan technique to a maximum 2θ value of 50.0° at a scan speed of 16.0°/min (in ω). The data were corrected for Lorentz and polarization effects.

The structure was solved by direct methods[8] and expanded using Fourier techniques.[9] The non-hydrogen atoms were anisotropically refined. Hydrogen atoms were included. Full-matrix least-squares refinement based on 2482 observed reflections ($I > 3.00\sigma(I)$) were employed, using the unweighted and weighted agreement factors $R = \sum||F_o| - |F_c||/\sum|F_o|$ and $R_w = [\sum w(|F_o| - |F_c|)^2/\sum w|F_o|^2]^{1/2}$. The weighting scheme was based on counting statistics. Plots of $\sum w(|F_o| - |F_c|)^2$ versus $|F_o|$, reflection order in data collection, $\sin\theta/\lambda$, and various classes of indices showed no unusual trends. Neutral atomic scattering factors were taken from Cromer and Waber.[10] Anomalous dispersion effects were included in F_{calcd}; the values $\Delta f'$ and $\Delta f''$ were those of Creagh and McAuley.[11] The values for the mass attenuation coefficients are those of Creagh and Hubbel.[12] All calculations were performed using the teXsan crystallographic software package of Molecular Structure Corporation.[13] Crystal data and details of the structure determinations are summarized in Table 1, and relevant bond distances and angles are listed in Table 2. The fragile nature of the crystals made it difficult to improve the quality of the X-ray analysis.

Table 1. Crystallographic Data for **5**

empirical formula	$C_{56}H_{56}Fe_4N_{12}O_{11}$
a, Å	13.495(7)
b, Å	14.220(9)
c, Å	33.137(5)
β, deg	96.74(2)
V, Å^3	6315(4)
Z	4
fw	1296.52
space group	$P2_1/n$ (No. 14)
t, °C	20
λ, Å	0.710 69
ρ_{calcd}, g cm^{-3}	1.364
μ, cm^{-1}	9.64
R^a	7.0
$R_w{}^b$	8.2

$^a R = \sum||F_o| - |F_c||/\sum|F_o|$. $^b R_w = [\sum w(|F_o| - |F_c|)^2/\sum w|F_o|^2]^{1/2}$, $w = 1/[\sigma^2(F_o)]$.

General Procedures and Materials. All chemicals and solvents used for the synthesis were reagent grade. The quadridentate Schiff base ligand H_2salen were synthesized by mixing salicylaldehyde and ethylenediamine in 2:1 mole ratio in ethanol, according to the literature procedure.[14] Iron(III) complex [Fe(salen)(Cl)], **1**, was prepared by mixing anhydrous iron(III) chloride and H_2salen in absolute methanol in the molar ratio of 1:1 according to a previously reported method.[15] $[NEt_4]_3[Fe(CN)_6]$ **2** was also prepared according to the literature.[16]

Preparation of 4. Since the hexacyanometalate ion has a tendency to decompose during heating and irradiation, the iron(III) complexes, **4** and **5**, were synthesized at room temperature and crystallized in a dark room. To a solution of **1** (0.18 g, 0.5 mmol) in methanol (50 mL) was added a solution of **2** (0.30 g, 0.5 mmol) in methanol (10 mL), and the resulting purplish-brown solution stirred at room temperature. Purplish-brown microcrystals precipitated and were collected by suction filtration, washed with a minimum volume of ethanol, and dried in vacuo. The micro- and thermogravimetry analysis showed that the compound contains one molecule of methanol as a crystal solvent per molecule per formula unit. Anal. Calcd for $C_{47}H_{52}N_{11}O_5Fe_3$: C, 55.42; H, 5.15; N, 15.13; Fe, 16.45. Found; C, 55.35;

(2) (a) Miller, J. S.; Epstein, A. J.; Reiff, W. M. *Chem. Rev.* **1988**, *88*, 201. (b) Nakatani, K.; Carriat, J. Y.; Journaux, Y.; Kahn, O.; Lloret, F.; Renard, J. P.; Pei, Y.; Sletten, J.; Verdaguer, M. *J. Am. Chem. Soc.* **1989**, *111*, 5739. (c) Kahn, O.; Pei, Y.; Verdaguer, M.; Renard, J. P.; Sletten, J. *J. Am. Chem. Soc.* **1988**, *110*, 782. (d) Caneschi, A.; Gatteschi, D.; Renard, J. P.; Rey. P.; Sessoli, R. *Inorg. Chem.* **1989**, *28*, 1976. (e) Caneschi, A.; Gatteschi, D.; Renard, J. P.; Rey, P.; Sessoli, R. *Inorg. Chem.* **1989**, *28*, 3314. (f) Caneschi, A.; Gatteschi, D.; Rey, P.; Sessoli, R. *Inorg. Chem.* **1991**, *30*, 3937. (g) Benelli, C.; Caneschi, A.; Gatteschi, D.; Sessoli, R. *Inorg. Chem.* **1993**, *32*, 4797. (h) Caneschi, A.; Gatteschi, D.; Sessoli, R. *Inorg. Chem.* **1993**, *32*, 4612. (i) Gatteschi, D. *Adv. Mater.* **1994**, 6, 635. (j) Caneschi, A.; Gatteschi, D.; Sessoli, R.; Rey, P. *Acc. Chem. Res.* **1989**, *22*, 392. (k) Caneschi, A.; Gatteschi, D.; Rey, P. *Progr. Inorg. Chem.* **1989**, *22*, 392. (l) Miller, J. S.; Epstein, A. J. *Angew. Chem., Int. Ed. Engl.* **1994**, *33*, 399. (m) Lorente, M. A. M.; Tuchagues, J. P.; Petrouleas, V.; Savariault, J. M.; Poinsot, R.; Drillon, M. *Inorg. Chem.* **1991**, *30*, 3587. (n) Stumpf, H. O.; Pei, Y.; Kahn, O.; Sletten, J.; Renard, J. P. *J. Am. Chem. Soc.* **1993**, *115*, 6738. (o) Stumpf, H. O.; Ouahab, L.; Pei, Y.; Grandjean, D.; Kahn, O. *Science* **1993**, *261*, 447. (p) Tamaki, H.; Zhong, Z. J.; Matsumoto, N.; Kida, S.; Koikawa, M.; Achiwa, N.; Hashimoto, Y.; Okawa, H. *J. Am. Chem. Soc.* **1992**, *114*, 6974. (q) Ohba, M.; Maruono, N.; Okawa, H.; Enoki, T.; Latour, J.-M. *J. Am. Chem. Soc.* **1994**, *116*, 11567. (r) Ohba, M.; Okawa, H.; Ito, T.; Ohto, A. *J. Chem. Soc., Chem. Commun.* **1995**, 1545. (s) Inoue, K.; Iwamura, H. *J. Am. Chem. Soc.* **1994**, *116*, 3173. (t) Grieber, W. D.; Babel, D. *Z. Naturforsch.* **1982**, *87B*, 832. (u) Gadet, V.; Mallah, T.; Castro, I.; Veillet, P.; Verdaguer, M. *J. Am. Chem. Soc.* **1992**, *114*, 9213. (v) Mallah, T.; Thiebault, S. Verdaguer, M.; Veillet, P. *Science* **1993**, *262*, 1555. (w) Mitra, S.; Gregson, A. K.; Hatfield, W. E.; Weller, R. R. *Inorg. Chem.* **1983**, *22*, 1729. (x) Martinez-Lorente, M. A.; Tuchagues, J. P.; Pétrouléas, V.; Savariault, J. M.; Poinsot, R.; Drillon, M. *Inorg. Chem.* **1991**, *30*, 3587.

(3) (a) Kahn, O. *Molecular Magnetism*; VCH: Weinheim, Germany, 1993. (b) Kahn, O. *Structure and Bonding*; Springer-Verlag: Berlin, 1987; Vol. 68. (c) Gatteschi, D., Kahn, O., Miller, J. S., Palacio, F., Eds. *Magnetic Molecular Materials*; NATO ASI Series E 198; Kluwer Academic: Dordrecht, The Netherlands, 1991. (d) Willett, R. D., Gatteschi, D., Kahn, O., Eds. *Magneto-Structural Correlations in Exchange Coupled Systems*; Nato ASI Series C 140; Kluwer Academic: Dordrecht, The Netherlands, 1985. (e) Miller, J. S.; Epstein A. J. *Angew. Chem., Int. Ed. Engl.* **1994**, *33*, 385. (f) Borrás-Almenar, J. J.; Coronado, E.; Curely, J.; Georges, R.; Gianduzzo, J. C. *Inorg. Chem.* **1994**, *33*, 5171. (g) Gleizes, A.; Verdaguer, M. *J. Am. Chem. Soc.* **1984**, *106*, 3727.

(4) (a) Sato, O.; Iyoda, T.; Fujishima, A.; Hashimoto, K. *Science* **1996**, *272*, 704. (b) Hinek, R.; Guetlich, P.; Hauser, A. *Inorg. Chem.* **1994**, *33*, 567.

(5) (a) Miyasaka, H.; Matsumoto, N.; Ōkawa, H.; Re, N.; Gallo, E.; Floriani, C. *Angew. Chem., Int. Ed. Engl.* **1995**, *34*, 1446. (b) *J. Am. Chem. Soc.* **1996**, *118*, 981. (c) Re, N.; Gallo, E.; Floriani, C.; Miyasaka, H.; Matsumoto, N. *Inorg. Chem.* **1996**, *35*, 5964. (d) Miyasaka, H.; Matsumoto, N.; Re, N.; Gallo, E.; Floriani, C. *Inorg. Chem.* **1997**, *36*, 670.

(6) Lindoy, L. F.; Katovic, V.; Busch, D. H. *J. Chem. Educ.* **1972**, *49*, 117.

(7) Boudreaux, E. A.; Mulay, L. N. In *Theory and Applications of Molecular Paramagnetism*; Wiley: New York, 1976; pp 491−495.

(8) Sheldrick, G. M. *SHELXS86*: *A program for X-ray crystal structure determination*; University of Cambridge: Cambridge, U.K., 1986.

(9) Beurskens, P. T.; Admiraal, G.; Beurskens, G.; Bosman, W. P.; Garcia-Granda, S.; Gould, R. O.; Smits, J. M. M.; Smykalla, C. *DIRDIF92: The DIRDIF program system*; Technical Report of the Crystallography Laboratory; University of Nijmegen: The Netherlands, 1992.

(10) Cromer, D. T.; Waber, J. T. *International Tables for Crystallography*; Kynoch: Birmingham, England, 1974; Vol. IV, Table 2.2A.

(11) Creagh, D. C.; McAuley, W. J. In *International Tables for Crystallography*; Wilson, A. J. C., Ed.; Kluwer: Boston, 1992; Vol. C, pp 219−222, Table 4.2.6.8.

(12) Creagh, D. C.; Hubbel, J. H. In *International Tables for Crystallography*; Wilson, A. J. C., Ed.; Kluwer: Boston, 1992; Vol. C, pp 200−206, Table 4.2.4.3.

(13) *teXsan: Crystal Structure Analysis Package*; Molecular Structure Corporation: The Woodlands, TX, 1985 and 1992.

(14) Pfeiffer, P.; Hesse, T.; Pfitzner, H.; Scholl, W.; Thielert, H. *J. Pract. Chem.* **1937**, *149*, 217.

(15) (a) Pfeiffer, P.; Breith, E.; Lübbe, E.; Tsumaki, T. *Liebigs Ann. Chem.* **1933**, *503*, 84. (b) Nishida, Y.; Oshio, S.; Kida, S. *Bull. Chem. Soc. Jpn.* **1977**, *50*, 119.

(16) Mascharak, P. K. *Inorg. Chem.* **1986**, *25*, 245.

Table 2. Relevant Bond Distances (Å) and Angles (deg) with the Estimated Standard Deviations in Parentheses for **5**[a]

Fe(1)−O(1)	1.886(8)	Fe(3)−N(8)	2.14(1)
Fe(1)−O(2)	1.890(8)	N(8)−C(36)	1.15(1)
Fe(1)−N(1)	2.07(1)	Fe(4)−C(36)	1.90(1)
Fe(1)−N(2)	2.11(1)	Fe(4)−C(37)	1.93(1)
Fe(1)−N(3)	2.08(1)	Fe(4)−C(38)	1.97(1)
Fe(1)−N(9)*	2.17(1)	N(9)−C(37)	1.15(1)
N(3)−C(17)	1.12(1)	N(10)−C(38)	1.11(1)
Fe(2)−C(17)	2.01(1)	Fe(5)−O(5)	1.94(1)
Fe(2)−C(18)	2.00(2)	Fe(5)−O(6)	1.877(10)
Fe(2)−C(19)	1.97(1)	Fe(5)−O(7)	2.12(1)
N(4)−C(18)	1.12(2)	Fe(5)−O(8)	2.12(1)
N(5)−C(19)	1.14(1)	Fe(5)−N(11)	2.15(1)
Fe(3)−N(5)	2.10(1)	Fe(5)−N(12)	2.11(1)
Fe(3)−O(3)	1.910(8)	O(7)−C(55)	1.74(4)
Fe(3)−O(4)	1.892(8)	O(8)−C(56)	1.44(3)
Fe(3)−N(6)	2.112(10)	hydrogen bond	
Fe(3)−N(7)	2.13(1)	O(8)−N(10)*	2.62(1)

Fe(1)−N(3)−C(17)	165(1)	Fe(4)−C(36)−N(8)	173(1)
Fe(2)−C(17)−N(3)	179(1)	Fe(4)−C(37)−N(9)	173(1)
Fe(2)−C(19)−N(5)	177(1)	Fe(1)−N(9)*−C(37)*	154(1)
Fe(3)−N(5)−C(19)	150(1)	Fe(5)−O(7)−C(55)	127(1)
Fe(3)−N(8)−C(36)	168(1)	Fe(5)−O(8)−C(56)	123(1)

[a] "*" refers to the equivalent position, x, $1 + y$, z; "**" refers to the equivalent position, $1/2 + x$, $1/2 - y$, $1/2 + z$.

H, 5.00; N, 15.47; Fe, 15.62. IR(KBr): $\nu_{C=N}$ (imine), 1597 and 1638 (broad) cm^{-1}; $\nu_{C\equiv N}$ (cyanide), 2124 and 2141 cm^{-1}. Mp: 218 °C.

Preparation of 5. To a stirred solution of **1** (0.18 g, 0.5 mmol) in methanol (50 mL) was slowly added a solution of **3** (0.165 g, 0.5 mmol) in water (20 mL) at room temperature. Stirring was then discontinued, and the solution was left for 2 days. The resulting dark purplish-brown thin plate crystals were collected by suction filtration, washed with a minimum volume of water, and dried in air. The micro- and thermogravimetric analyses showed that the compound contains two methanol molecules as solvent ligands and three water molecules as solvents of crystallization per formula unit. Three of the water molecules were easily eliminated by drying in vacuo or heating. The magnetic properties of the dehydrated compound are different from the parental compound. Therefore, the single crystals for X-ray crystallographic analysis and magnetic measurements were carried out under conditions which avoided efflorescence. Anal. Calcd for $C_{56}H_{50}N_{12}O_8Fe_4$: C, 54.14; H, 4.06; N, 13.53; Fe, 17.98. Found: C, 53.75; H, 3.67; N, 13.91; Fe, 14.64. IR(KBr): $\nu_{C=N}$ (imine), 1599, 1618 (broad), and 1636 (broad) cm^{-1}; $\nu_{C\equiv N}$ (cyanide), 2025 (broad), and 2077 cm^{-1}. Mp: 218 °C.

Results and Discussion

Synthesis and Characterization. The assembling of the high-spin d^5 $[Fe(salen)]^+$ with the low-spin d^5 $[Fe(CN)_6]^{3-}$ has been achieved by reacting [Fe(salen)(Cl)], **1**, with $A_3[Fe(CN)_6]$ (A = NEt_4, **2**; A = K, **3**] in polar solvents. Two structurally related compounds have been obtained depending on the countercation A^+ and the reaction solvent, as reported in Scheme 1. An X-ray analysis of **5** (vide infra) clarified its structure and along with the corresponding magnetic measurements established the structural relationship with **4**. Both compounds give rise to the same 2D layer structure containing the same repeating octanuclear ring unit as shown in Scheme 1. The only difference between the two concerns the countercation filling the interlayer space. In the case of **4** this is NEt_4^+ cation, while for **5** the countercation $[Fe(salen)(MeOH)_2]^+$ is hydrogen bonded to the CN^- groups not involved in the 2D network. The overall $[Fe(salen)]^+/Fe(CN)_6]^{3-}$ ratio, though the basic structure is the same, is 2:1 and 3:1 for **4** and **5**, respectively. In the latter case, however, the additional $[Fe(salen)]^+$ cation does not play any important structural and magnetic role, it is just a noninteracting countercation.

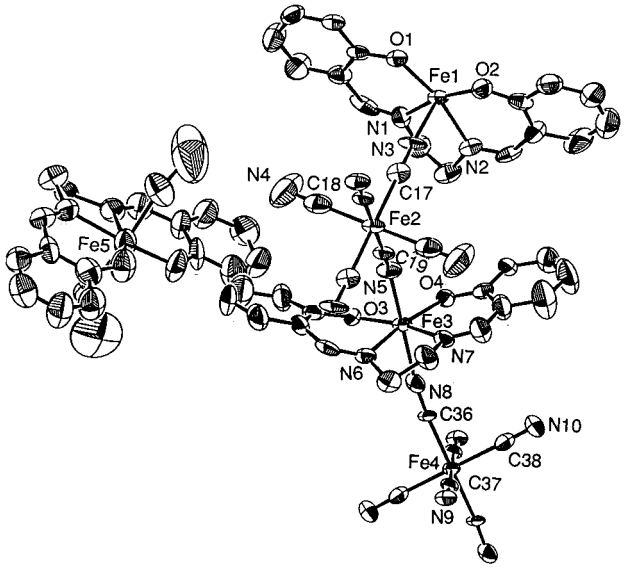

Figure 1. ORTEP drawing of **5** with the atom numbering scheme of the unique atoms, showing 50% probability ellipsoids and three water molecules as the crystal solvents are omitted for clarity, where Fe2 and Fe4 atoms have an occupancy of half-weight because of the inversion center.

Scheme 1

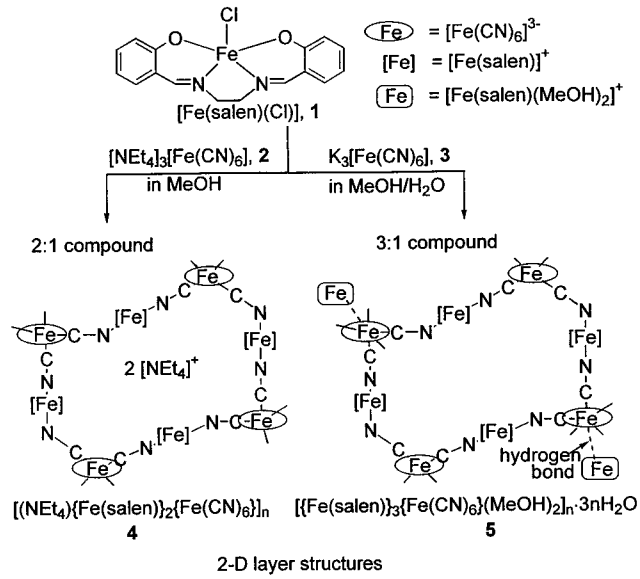

5 instead of **4** is obtained, due both to the role of $K_3[Fe(CN)_6]$ and to the presence of H_2O in methanol which favors the ionization of the Fe−Cl bond in **1**. The thermogravimetric analysis confirmed that in compound **4** methanol is loosely held in the structure, whereas it is strongly bonded to iron in $[Fe(salen)(MeOH)_2]^+$ (complex **5**). This is further supported by the X-ray analysis. In the latter case, the water of crystallization is easily lost above 37 °C.

Structural Analysis of 4 and 5. Since **5** crystallizes in the monoclinic space group $P2_1/n$ with $Z = 4$, a formula consisting of $[\{Fe(salen)\}_3\{Fe(CN)_6\}(MeOH)_2]\cdot 3H_2O$ is a crystallographic unique unit. An ORTEP view of the unique unit with the atom numbering scheme is shown in Figure 1, in which two iron atoms of $[Fe(CN)_6]^{3-}$, Fe2 and Fe4, occupy the special positions with a half weight at ($^1/_2$, $^1/_2$, 0) and (0, 0, 0), respectively, and the other iron atoms occupy the general positions. Four iron moieties, Fe1, Fe2, Fe3, and Fe4, form a two-dimensional network structure (see Figure 2a) consisting of a cyclic

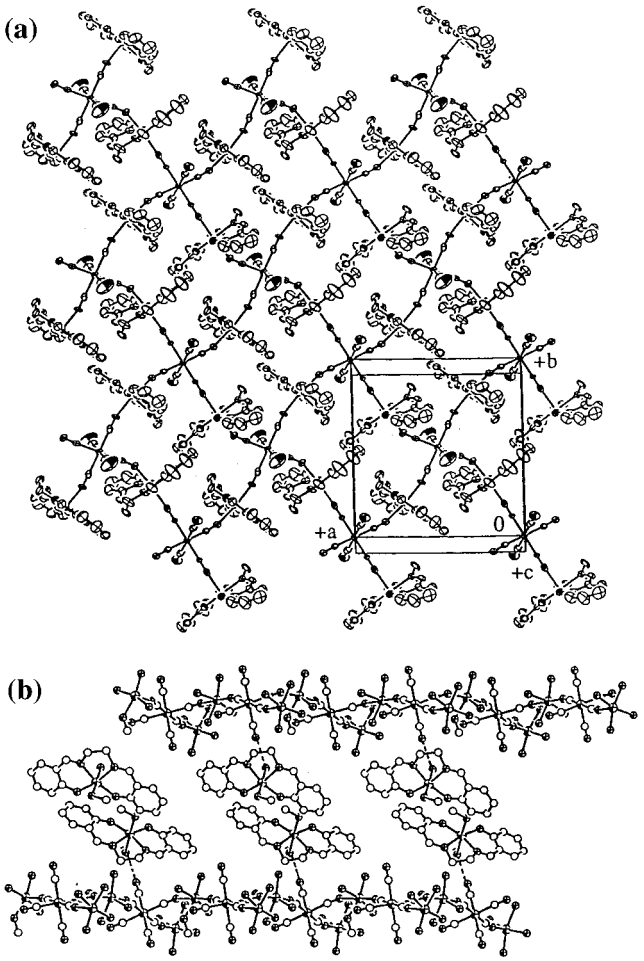

Figure 2. (a) Two-dimensional network structure of **5** comprising a cyclic octanuclear net unit [-Fe1-NC-Fe2-CN-Fe3-NC-Fe4-CN-]$_2$. (b) Formation of the hydrogen bond between the two-dimensional layer and [Fe(salen)(MeOH)$_2$]$^+$, where the hydrogen bonds appear at both sides of the layer (upside and downside) against the inversion center Fe4 (O8···C38-Fe4-C38′-N10′···O8′) and once at every other [Fe(CN)$_6$]$^{3-}$ moiety of octanuclear net unit [-Fe1-NC-Fe2-CN-Fe3-NC-Fe4-CN-]$_2$.

octanuclear unit [-Fe1-NC-Fe2-CN-Fe3-NC-Fe4-CN-]$_2$ as a net unit, and the remaining Fe5 moiety plays the role of counter-cation, with [Fe(salen)(MeOH)$_2$]$^+$ hydrogen bonded via the methanol proton to one of the nitrogens of the [Fe(CN)$_6$] moiety of the layer (Figure 2b). All three Fe(III) salen moieties have an octahedral coordination geometry in which the equatorial sites are occupied by the N_2O_2 quadridentate salen Schiff base ligand.

The two-dimensional network structure of **5** is similar to that of metamagnet K[Mn(3-MeOsalen)]$_2$[Fe(CN)$_6$](DMF),[5a,b] and the ferrimagnet [NEt$_4$][Mn(5-Clsalen)]$_2$[Fe(CN)$_6$][5d] reported previously. The interlayer distance of the present compound, 16.57 Å, is much longer than in K[Mn(3-MeOsalen)]$_2$[Fe(CN)$_6$]-(DMF), 13.75 Å, and [NEt$_4$][Mn(5-Clsalen)]$_2$[Fe(CN)$_6$], 13.10 Å, due to the presence of [Fe(salen)(MeOH)$_2$]$^+$, rather than the smaller DMF or NEt$_4^+$ as spacer between two adjacent layers.

Even though an X-ray analysis is not available, the structure of **4** can be very reasonably inferred from that of **5** and by analogy with the Mn analogues.[5] In the case of **4**, we believe that the interlayer space is filled by NEt$_4^+$ cations. This hypothesis is supported by the magnetic data which clearly indicate a metamagnetic behavior characteristic of a layer structure (vide infra).

Magnetic Properties of 4. The magnetic susceptibility was measured from 1.9 to 300 K and the plots of μ_{eff} vs T and $1/\chi_M$ vs T for the compound are given in Figure 3. The plots of $1/\chi_M$ vs T above 30 K obey the Curie−Weiss law with a positive Weiss constant of $\theta = +2.5$ K, indicating the presence of a weak ferromagnetic interaction. The μ_{eff} at room temperature, 9.72 μ_B at 298 K, is slightly higher than the spin-only value of 8.72 μ_B expected for the magnetically dilute spin system (S_{Fe}(h.s.), S_{Fe}(l.s.), S_{Fe}(h.s.)) = ($^5/_2$, $^1/_2$, $^5/_2$), where the spin-only value was calculated by assuming g_{Fe}(l.s.) = g_{Fe}(h.s.) = 2.00. On lowering the temperature, the μ_{eff} increases gradually, then abruptly to reach a maximum of 33.1 μ_B at 10.1 K, and finally decreases sharply to 21.7 μ_B at 1.9 K. These behaviors suggest an intralayer ferromagnetic interaction between the high-spin Fe(III) component of [Fe(salen)] and the low-spin Fe(III) component of [Fe(CN)$_6$]$^{3-}$ via bridging CN groups.

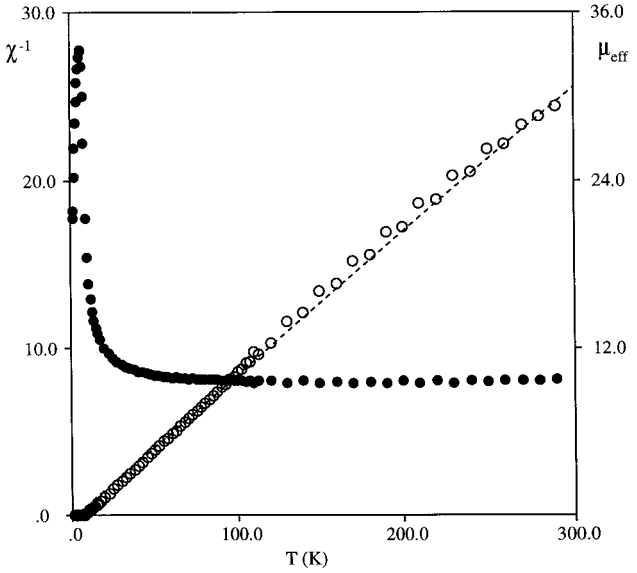

Figure 3. Plots of the effective magnetic moment μ_{eff} and $1/\chi_M$ per Fe_2Fe unit vs T for **4**.

The abrupt increase of μ_{eff} below 30 K to a value much higher than that of the largest possible spin state ($S_T = 11/2$, $\mu_{eff} = 11.96\ \mu_B$) suggests the onset of magnetic ordering. To confirm the magnetic phase transition, the FCM (field cooled magnetization), RM (remnant magnetization), and ZFCM (zero-field cooled magnetization) curves vs T were measured under zero and weak magnetic field of 3 Oe and are given in Figure 4. When the temperature is lowered, the FCM curve under 3 Oe shows a rapid increase below ca. 8 K to reach a broad maximum around 6 K, and then decreases further. When the field was switched off at 1.9 K, an RM was observed upon warming which is initially almost superimposable to the FCM curve. The ZFCM vs T curve was obtained by cooling the sample under zero field and warming it under 3 Oe. The ZFCM shows a peak at ca. 6 K and then disappears on warming. The abrupt increase of the magnetization below ca. 8 K in the FCM curve indicates the onset of long-range magnetic ordering due to the ferromagnetic coupling within each layer. The decrease below 6 K indicates the presence of interlayer antiferromagnetic interactions. Note that both the RM and ZFCM curves show a discontinuity with a large decrease at 4.2 K. This is probably because of the fast dynamics of domain walls at this temperature at which, due to the instrumental switch between the two different regimes below and above helium liquefaction temperature, the compound is kept for a longer time. To further investigate this point, we measured FCM curves at 150, 300, and 500 Oe (see Figure 5). We see that while under a field of 300 Oe or lower the magnetization still shows a peak at 6 K,

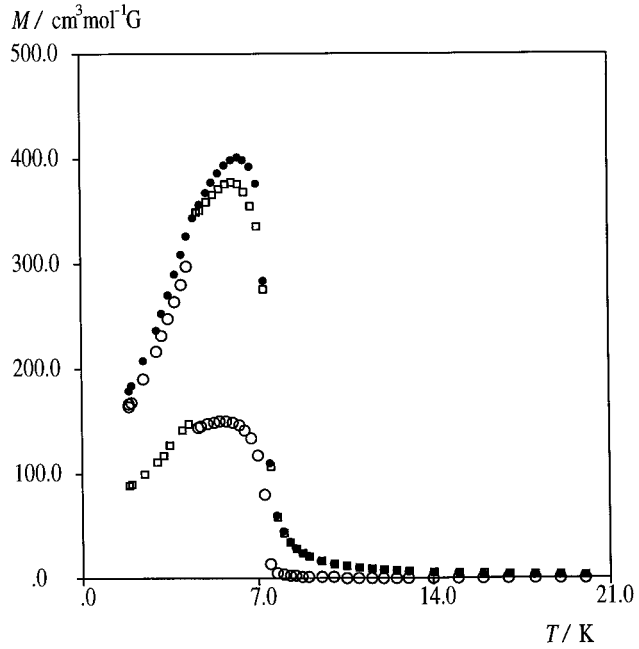

Figure 4. FCM (field cooled magnetization vs *T*, ●) curve under 3 Oe, RM (remnant magnetization vs *T*, ○), and ZFCM (zero-field cooled magnetization, □) for **4**.

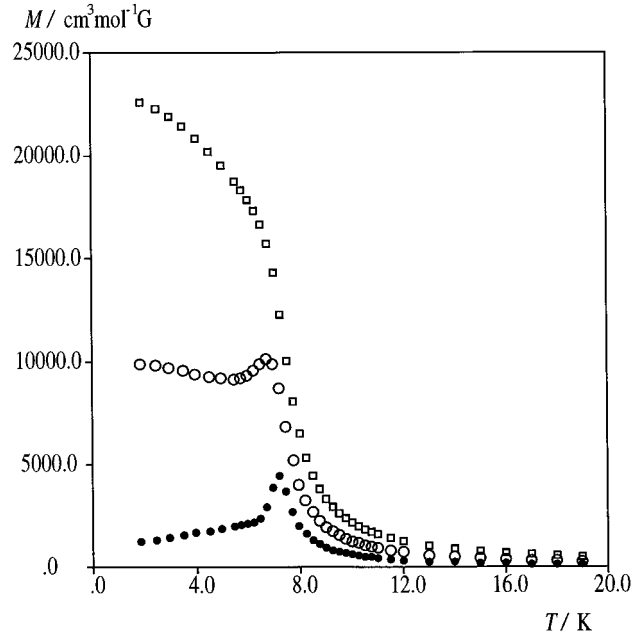

Figure 5. FCM (field cooled magnetization vs *T*) curve under 100 Oe (●), 300 Oe (○) and 500 Oe (□) for **4**.

the curve under 500 Oe has no peak and saturates below the abrupt increase at ca. 8 K. This implies that a field of 500 Oe or higher can overcome the weak interlayer interaction orienting in a parallel fashion the layer magnetic vectors. These data demonstrate that the complex is a metamagnet.[17] To better characterize the metamagnetic transition, the magnetization was measured as a function of the external magnetic field at various

(17) (a) Carlin, R. L. *Magnetochemistry*; Springer-Verlag: Berlin, Germany, 1986. (b) Kahn, O. In *Magneto-Structural Correlations in Exchange Coupled Systems*; Gatteschi, D., Kahn, O., Willett, R. D., Eds.; Reidel: Dordrecht, The Netherlands, 1985; pp 37−56. (c) Carlin, R.; vanDuyneveldt, A. *Acc. Chem. Res.* **1980**, *13*, 231. (d) De Fotis, G. C.; McGhee, E. M.; Bernal, I.; Losee, D. B. *J. Appl. Phys.* **1987**, *61*, 3298. (e) Smart, J. S. *Effective Field Theories of Magnetism*; Saunders: Philadelphia, 1966.

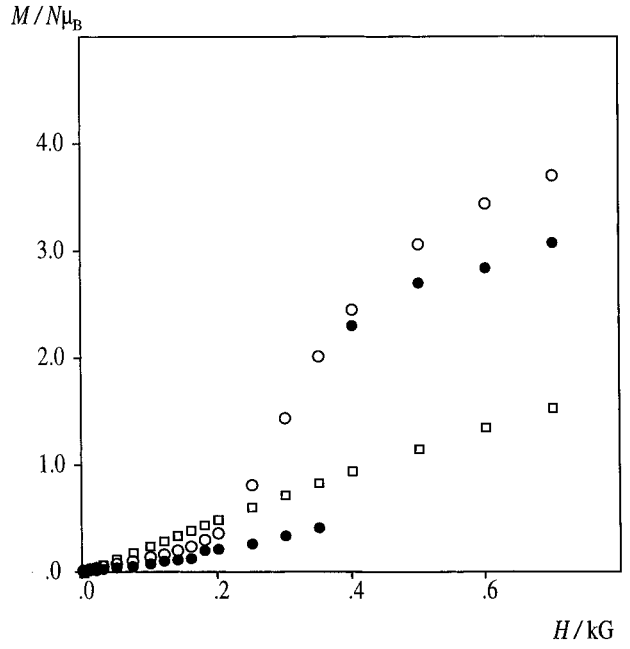

Figure 6. Magnetization as a function of the applied magnetic field up to 1 kOe for **4** at 1.9 K (●), 6 K (○), and 8 K (□).

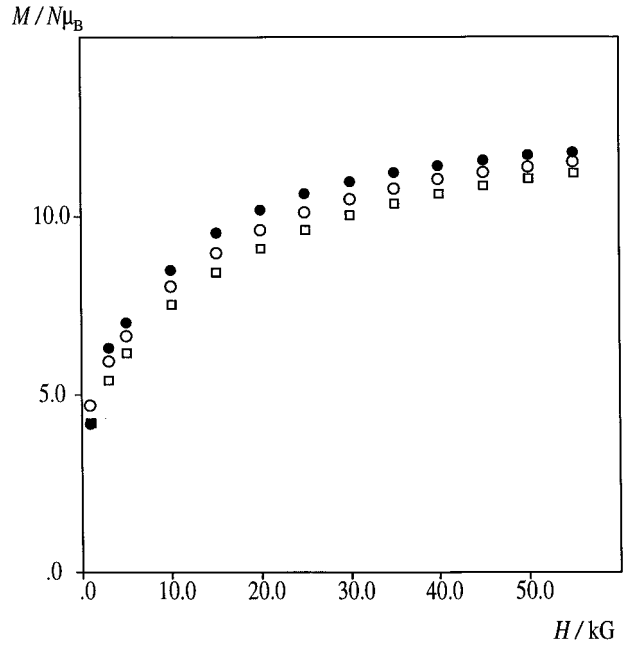

Figure 7. Magnetization as a function of the applied magnetic field for **4** up to 55 kOe at 1.9 K (●), 4 K (○), and 6 K (□).

temperatures below and above the Neel temperature (see Figure 6). Below 6 K the curves show a sigmoidal behavior: the magnetization first increases slowly with the field as for a typical antiferromagnet and then increases abruptly showing a phase transition to a ferromagnetic state, as expected for a metamagnet. The critical field (the lowest field which is able to reverse the interlayer antiferromagnetic interaction) is ca. 350 Oe at 1.9 K; as the temperature is raised, the phase transition shifts to lower field and then disappears for temperatures above 6 K, still confirming the metamagnetic transition.

The field dependence of the magnetization up to 55 kOe was measured at 1.9, 4.5, and 6 K, and the results are shown in Figure 7. The curve at 1.9 K increases rapidly after 400 Oe with an extremely large zero-field susceptibility (i.e., a very weak magnetic field is sufficient to induce a large magnetization)

and then more gradually to almost reach saturation at the highest measured field (55 kOe). The corresponding value of 11.8 Nμ_B is only slightly higher than the expected saturation value of 11 Nμ_B [$= 2 \times (2 \times {}^5/_2 + {}^1/_2)$]. This behavior is quite different from that observed for the structurally related series of 2D magnetic materials previously reported,[5] for which the saturation was far from being reached at 55 kOe. This is easily explained if we consider that all those materials were based on the strongly anisotropic high-spin d^4 [Mn(Schiff base)] unit, which caused the magnetization to increase more slowly than is forecast by the corresponding Brillouin function, while **4** is based on the essentially isotropic high-spin d^5 [Fe(salen)] unit.

Magnetic Property of 5. The magnetic properties of **5** above 20 K can be interpreted as the superimposing of the magnetic properties of $[Fe(salen)]_2[Fe(CN)_6]$ two-dimensional network and that of the noninteracting $[Fe(salen)](MeOH)_2]^+$ countercations. Although we do not discuss this in detail here, it is sufficient to say that at lower temperatures the magnetic properties are determined by the interlayer interactions and, due to the presence of loosely bound $[Fe(salen)](MeOH)_2]^+$ units and water molecules as layer spacers, are very sensitive to sample drying condition and aging.

For typical freshly prepared samples, the plots of $1/\chi_M$ vs T above 30 K obey the Curie−Weiss law with a small positive Weiss constant of $\theta = +2.0$ K, indicating the presence of a weak ferromagnetic interaction. The temperature dependence of μ_{eff} is analogous to that of **4**, but the values of the magnetic moment at the maxima around 10 K and at 1.9 are strongly dependent on sample drying condition and aging and are barely reproducible. These values are, however, in the range 14−17 μ_B and therefore much lower than the value observed for **4**. The FCM curves measured for **5** at 3 Oe show a rapid increase below ca. 8 K, still indicating the onset of a magnetic ordering, and then show further increases down to 1.9 K without any maximum, as for **4**. This latter behavior does not indicate, at variance with **4**, any antiferromagnetic interaction so that **5** could order ferromagnetically.

The field dependence of the magnetization up to 55 kOe, measured at 1.9 K, do not show any sigmoidal behavior and reaches an almost complete saturation with a value of 14.9 Nμ_B per Fe_3(h.s)Fe(l.s.) unit close to the expected saturation value [16 N$\mu_B = 2 \times (3 \times {}^5/_2 + {}^1/_2)$] for intralayer ferromagnetic interactions.

Magneto-Structural Correlation. In a simple orbital scheme of exchange between two magnetic centers,[18] e.g. A and B, the coupling constant J can be given by the sum of several pair contributions due to the interaction between the magnetic orbitals on center A and those on B. These pair contributions can be written as the sum of a ferromagnetic and an antiferromagnetic term; the latter term arises from the overlap integral between the two orbitals and usually dominates the former one, so that an overall ferromagnetic interaction is observed only if all magnetic orbitals on center A are orthogonal to those on B.

The magnetic interaction of two metal centers through a CN^- bridge in the Prussian blue family has been addressed both theoretically and experimentally along these lines.[19] If a similar analysis is applied to the CN^- bridged Fe(III) l.s.−Fe(III) h.s. interaction (low-spin d,[5] t_{2g}^5, high-spin d^5, $t_{2g}^3e_g^2$) in **4** and **5**, it would suggest the co-existence of both ferromagnetic and antiferromagnetic contributions and therefore an overall antiferromagnetic coupling, at variance with the observed small ferromagnetic interaction. Indeed, both ions have magnetic orbitals of t_{2g} symmetry which overlap, giving rise to antiferromagnetic contributions. Weak ferromagnetic coupling has already been observed in some $[\{Mn(BS)\}_2\{Fe(CN)_6\}]_n$ complexes for the CN^- bridged Fe(III) l.s.−Mn(III) h.s. interaction (d^5, t_{2g}^5; d^4, $t_{2g}^3e_g^1$), which is expected to be antiferromagnetic on the basis of the same analysis. Such an unexpected result was already explained in terms of a reduced overlap between the t_{2g} orbitals (d_{xz} and d_{yz}, taking the z axis along the Fe−Mn direction) due to a different orientation of the local ligand fields around the two metal centers.[20] We should also mention that the above ferromagnetic interaction is the result of a subtle compromise between opposite ferromagnetic and antiferromagnetic contributions so that small changes in the M−C−N−M′ geometry could lead to significant changes and even to an inversion of the magnetic coupling between the two ions, as already observed in $[(NEt_4)\{Mn(5\text{-}Clsalen)\}_2\{Fe(CN)_6\}]_n$.[5d]

It is also interesting to consider the origin of the magnetic ordering and the nature of the interlayer interactions in **4** and **5**. While a clear antiferromagnetic interaction operates between adjacent planes in **4**, as shown by the decrease of the FCM curve below 6 K, the situation is less clear in **5**. Both a negligible magnetic interaction or a weak ferromagnetic interaction could operate in the latter compound, and only further magnetic measures below 1.9 K could allow to distinguish between the two possibilities. However, the large interlayer separation observed in **5** (16.57 Å), much larger than that expected for **4** on the basis of the analogy with previously characterized compounds[5a,b,d] (13−14 Å), and the lack of contacts between the magnetic countercation hydrogen bonded to adjacent planes (see Figure 2b) would suggest the former possibility, i.e. a negligible interlayer magnetic interaction. The lack of structural data for **4** prevents any conclusion on the origin of the interlayer interaction in this compound. The analogy with previously characterized compounds[5a,b,d] suggests, however, exchange interactions through the countercation, probably via van der Waals contacts.

The magnetic nature of **4** and **5** would therefore be determined by the extent of the interplane interaction: metamagnetism when there is a significant interlayer antiferromagnetic interaction, as in **4**, or essentially 2D ferromagnetism when the interlayer magnetic interaction is negligible, as in **5**.

Acknowledgment. This work was supported by the JSPS Research Fellowships for Young Scientists (H.M.). Foundation Herbette (University of Lausanne, N.R.) and Fonds National Suisse de la Recherche Scientifique (Bern, Switzerland) are also acknowledged for financial support.

Supporting Information Available: X-ray structure report, experimental details, atomic coordinates, anisotropic displacement parameters, and complete lists of bond distances and angles for **5** are available (21 pages). Ordering information is given on any current masthead page.

IC971544D

(18) (a) Anderson, P. W. In *Magnetism*; Rado, G. T., Suhl, H., Eds.; Academic: New York, 1963; Vol. 1, p 25. (b) Goodenough, J. B. *Magnetism and the Chemical Bond*; Wiley: New York, 1963. (c) Hay, P. J.; Thiebault, J. C.; Hoffmann, R. *J. Am. Chem. Soc.* **1975**, *97*, 4884. (d) Kahn, O. In *Magneto-Structural Correlations in Exchange Coupled Systems*; Gatteschi, D., Kahn, O., Willett, R. D., Eds.; Reidel: Dordrecht, The Netherlands, 1985; p 37.

(19) Mallah, T.; Thiebault, S. Verdaguer, M.; Veillet, P. *Science* **1993**, *262*, 1555.

(20) See discussion in ref 5b.